Magnetite in hydrothermal orebodies and host rocks in the Proterozoic Belt Supergroup

Final Technical Report

PhD Student: Patrick Nadoll

Principal Investigator: Jeffrey L. Mauk

School of Geography, Geology and Environmental Science, The University of Auckland, Private Bag 92019, Auckland, J.Mauk@auckland.ac.nz

Award number: 06HQGR0173

Research supported by the U.S. Geological Survey (USGS), Department of the Interior, under USGS award number 06HQGR0173. The views and conclusions contained in this document are those of the authors and should not be interpreted as necessarily representing the official policies, either expressed or implied, of the U.S. Government.

Table of contents

Abstract

Magnetite (Fe_3O_4) is a common and widespread accessory mineral in greenschist facies Middle Proterozoic metasedimentary rocks of the Ravalli Group of the Belt Supergroup in the western USA, a local accessory mineral in sediment-hosted stratiform copper deposits in western Montana and a rare mineral in mesothermal veins of the Coeur d'Alene mining district in northern Idaho. Electron microprobe analyses show that magnetite from all three occurrences – host rock, sediment-hosted copper, and mesothermal veins – is essentially pure Fe_3O_4; we did not detect any significant deviation from stoichiometric magnetite for samples from any of the three occurrences. This suggests that either magnetite formed as a stoichiometric mineral in all three occurrences, or that its chemistry was reset during subsolidus reequilibration during metamorphism. Oxygen isotope geothermometry between magnetite and carbonates from the sediment-hosted copper and mesothermal vein deposits yield metamorphic temperatures of c. 350-400°C. Laser ablation inductively coupled mass spectrometry analyses show subtle differences in trace element contents of magnetite from different geological environments, and therefore the geochemistry of magnetite, which is a common and widespread restite mineral in stream sediments, might provide a useful inventory of the rock types and mineral deposits that occur within a stream drainage.

Objectives

This research had three specific objectives.

(1) Test whether existing aeromagnetic data can be used to help delineate orebodies and altered rocks in the Belt Supergroup. To accomplish this objective, we will prepare maps that show both total magnetic intensity and analytic signal, so that we can compare these results with the mapped distribution of (a) former redbeds of the Ravalli Group, (b) known locations of "albite alteration zone" rocks, and (c) known occurrences of sediment hosted stratiform copper deposits and Coeur d'Alene veins.

(2) Test whether magnetite from (a) host rocks, (b) altered rocks, and (c) orebodies has distinctly different geochemical signatures. To accomplish this objective, we will obtain microprobe and laser ablation inductively coupled plasma-mass spectrometry (LA-ICP-MS) data of magnetite from well-characterized samples from each of the above environments.

(3) Determine the temperature of formation of magnetite in different occurrences using oxygen isotope analyses of coexisting oxide-silicate and/or oxide-carbonate mineral pairs.

We have accomplished all three objectives. This report focuses primarily on Objectives two and three, as these formed the core of our research activities.

Summary of Results

Aeromagnetic work

Data Source

Aeromagnetic data across the project area were acquired from the North American Magnetic Anomaly digital database (NAMAG, 2002a). This database is the product of a cooperative effort between the United States, Canadian and Mexican government agencies and comprises publicly available airborne and marine magnetic data. These data are primarily made up from government-flown surveys but also include proprietary surveys where available.

Magnetic data across the United States were compiled by the USGS from surveys collected in digital format and digitized data from contour maps where digital data did not exist. These digital and digitized datasets were processed to produce grids of individual surveys at 500 meter and 1000 meter grid cell sizes at an equivalent draped terrain clearance of 305 meters (1000 feet) (NAMAG, 2002b). Final grids were subsequently merged to form a nationwide, and ultimately continent-wide, grid of magnetic data.

Data Processing

Digital data of the total magnetic intensity (TMI) were acquired for the project area in the form of point data derived from the North American Magnetic Anomaly grid (NAMAG, 2002a). These data were converted into the NAD27 UTM Zone 11N projection providing a regular grid of data across the region at 1.06 kilometer spacing. The TMI data were then gridded using the minimum curvature method to a cell size of 250 meters.

A reduced-to-pole grid of the data was calculated using International Geomagnetic Reference Field Tenth Generation (IGRF10) values at the centre of the project area based on the average date of the surveys comprising the dataset (IAGA, 2005). This was calculated as September 1969 at which time the IGRF had a declination of 20.164 degrees, inclination of 71.856 degrees and a total magnetic field intensity of 58000.63 nT.

The first and second vertical and total horizontal derivatives of both the TMI and RTP grids were calculated. In addition, the analytic signal of the TMI and tilt derivative of the RTP grids were determined.

A suite of digital images were produced for interpretation. These comprised linear and non-linear color stretches, greyscale, AGC filtered and unshaded and shaded versions of the TMI and RTP data and their derivatives. GIS compatible maps were given to the “Metallogenesis of Proterozoic Basins” team in Spokane in 2006.

Results

Aeromagnetic data from western Montana and northern Idaho, USA, closely correlate with regional geology. Magnetite produces the strongest and most abundant magnetic anomalies, which mainly reflect the locations of plutonic igneous rocks and Proterozoic Belt Supergroup strata. Plutonic igneous rocks show intense local

anomalies where small-scale plutons intrude older rocks, and broad anomalies over batholiths. For example, the twin plutons of the Rainy Creek igneous complex that outcrop immediately north and east of Libby produce distinct magnetic anomalies. The Rainy Creek igneous complex is an ultramafic laccolith with a biotitic core surrounded by biotite pyroxenite and magnetite pyroxenite that produces a magnetic anomaly with an amplitude greater than 6,000 nT (Boetcher, 1967; Kleinkopf, 1997; Harrison and Cressman, 1993). The complex hosts the largest vermiculite deposit in the world, which was mined from around 1920 to 1990 (e.g. Meeker et al., 2003, and references therein).

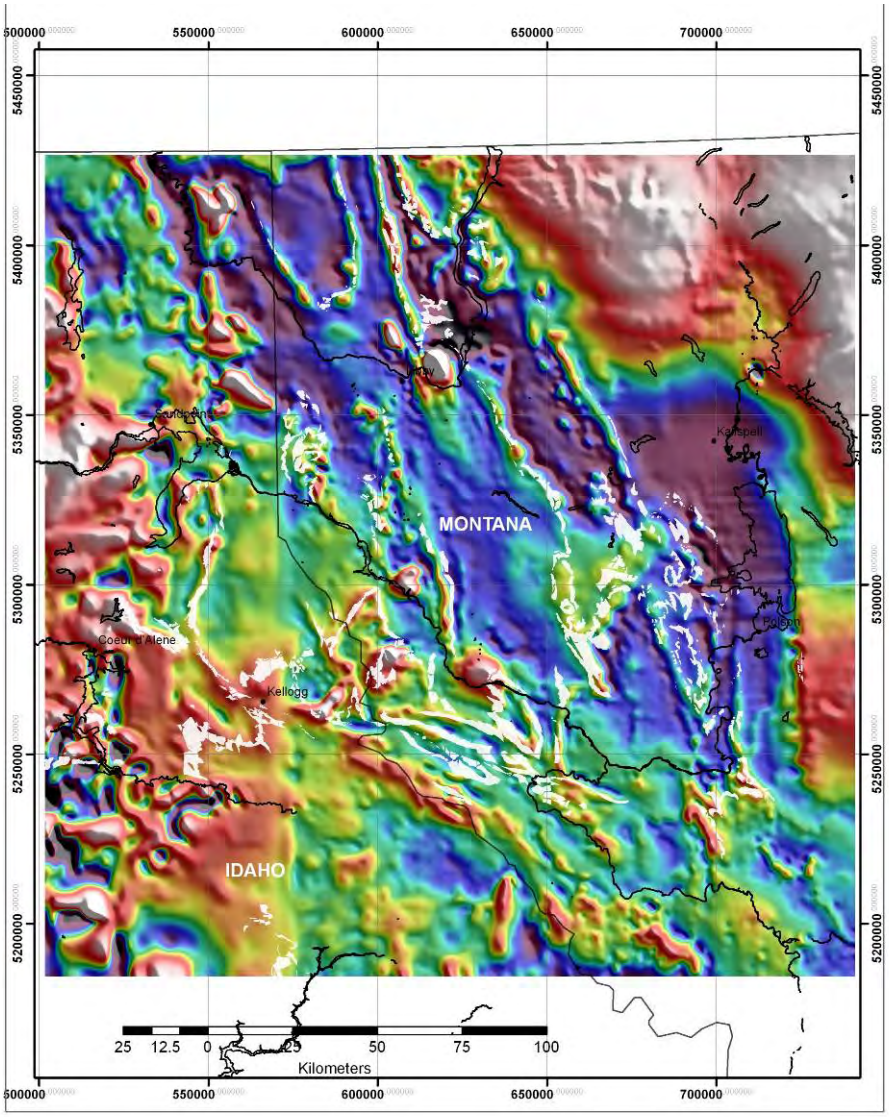

Figure 1. Total magnetic intensity map of western Montana and northern Idaho, showing positive anomalies associated with igneous intrusions and linear belts of high magnetic intensity that are associated with the map pattern of the Ravalli Group. Mapped area of the Revett Formation is shown by the extent of the cream unit that is draped over the TMI image.

Linear magnetic anomalies correlate closely with Proterozoic Belt Supergroup stratigraphy. The oldest Proterozoic rocks, the lower Belt, locally contain pyrrhotite,

but lack magnetite due to the overall reduced nature of the strata. The presence of pyrrhotite and the local sills indicate that high resolution magnetic surveys might provide an important tool to refine and improve geologic mapping of the lower Belt. However, at the scale of the surveys that we report, magnetic data do not significantly enhance resolution of lower Belt strata.

In contrast, rocks of the overlying Ravalli Group commonly contain magnetite, due to their original provenance as red beds, and because burial metamorphism of the Belt Supergroup has largely transformed original red bed hematite to magnetite. Neither the middle Belt carbonate interval nor the Missoula Group produce magnetic anomalies; the former because the strata are chemically reduced, and the latter because red beds in the Missoula Group have not been metamorphosed to sufficient rank to produce abundant magnetite.

In general, the linear magnetic anomalies that correlate with Ravalli Group rocks are more intense to the north and west of Libby, and of lower magnitude to the east. This correlates with the abundance and grain size of magnetite in the rocks. Magnetite is relatively abundant and coarse-grained in the Revett Formation to the north and west of Libby, but relatively minor and much finer-grained to the east. Although this may reflect regional differences in the original sedimentary and diagenetic constituents of these rocks, it might alternatively reflect variable metamorphic rank of different Ravalli Group rocks across different thrust sheets within the Belt terrane (Harrison et al., 1980).

The aeromagnetic data clearly reveal the structural setting of Ravalli Group rocks. For example, the Yaak River anticline north of Libby has a clear magnetic expression, as lower Belt rocks in the core of the anticline have low magnetic susceptibilities, whereas rocks of the Ravalli Group define a pronounced magnetic anomaly. In detail, the magnetic anomaly does not match the geologic mapping. In most places, the magnetic anomaly correlates with outcrops of Revett and/or Burke formations, however, in places the anomaly correlates with outcrops that have been mapped as St Regis Formation. This discrepancy suggests that magnetic susceptibility varies within formations, or that stratigraphic units have locally been mapped incorrectly, or a combination of these two.

Most areas of the Ravalli Group show prominent magnetic signatures for large strike lengths. However, in the area of the western Montana copper sulfide belt, the magnetic signature of the Ravalli Group, and particularly the Revett Formation is far more irregular and discontinuous. We interpret this lack of continuity as reflecting destruction of iron oxides, magnetite and hematite, during diagenetic reduction of the sediments. In part, this may be related to migration of hydrocarbons through Belt Supergroup stratigraphy, which can produce widespread chemically reduced horizons within sediments that were originally chemically oxidized. The discontinuous nature of the magnetic signature in the western Montana copper sulfide belt is therefore potentially useful for exploration, but more detailed analysis at the prospect level would be necessary to confirm this.

Geochemistry of magnetite

Most of our work has focused on the geochemistry of magnetite. This included sampling, detailed petrographic work, electron microprobe analyses, and laser-ablation ICP analyses.

Sampling

We collected a total of 98 magnetite-bearing samples from four geologic settings: (1) Samples from hydrothermally altered wall rocks and the hydrothermal veins of the Goldhunter mine in the Coeur d'Alene mining district. (2) Samples from burial metamorphic Revett Formation. (3) Samples from the sediment-hosted stratiform copper deposits of Rock Creek-Montanore and Troy (Spar Lake) (4) Samples from two igneous intrusions: (a) the hydrothermally altered and extensively weathered alkaline-ultramafic igneous intrusion at Rainy Creek, and (b) a granitic intrusion at Vermillion River, the Twenty-Odd Stock, which is associated with the emplacement of the Idaho Batholith to the west.

Petrography

Magnetite in the Belt Supergroup commonly occurs as disseminated subhedral to euhedral porphyroblasts. However, the magnetite found in the different localities and host rocks varies in size, and degree of alteration. Our field sampling indicated that alteration of magnetite, as represented by the increasing occurrence of martite (hematite after magnetite), increases from NW to SE, and can be observed in the field by careful examination. Increasing alteration is accompanied by a general decrease in magnetite grain size, from mm-scale porphyroblasts at Lake Koocanusa and in the Coeur d'Alene district to microscopic (<100 μm) grains in the Flathead area. Most samples show alteration to hematite (martite), which occurs along edges, fissures, cracks, and parallel to the octahedral (spinel) planes of the magnetite grains. In some samples, martite has completely replaced the magnetite, leaving behind hematite pseudomorphs after magnetite. Other grains show a more complex mixture of fine-grained oxidation products after magnetite and gangue.

Ilmenite ($FeTiO_3$) occurs in magnetite samples from the Rainy Creek pluton. It is oriented parallel to the magnetite octahedral planes showing different textures ranging from laths and lamellae to trellis.

In the sediment-hosted stratiform copper deposits, magnetite grains are generally less than 200 μm across, and occur as disseminated grains as well as in ore clots. Magnetite is commonly associated with copper sulfides such as chalcocite, bornite, chalcopyrite, enargite and pyrite. In some places, chalcocite and bornite form complete pseudomorphs after magnetite. The gangue material in these samples consists predominantly of quartz, serecite, alkali feldspar, microcline, plagioclase, calcite and chlorite. Hematite occurs in most samples, along fissures, cracks, and parallel to the octahedral spinel planes.

The Coeur d'Alene district host rocks contain euhedral magnetite porphyroblasts that are up to 500 μm across. Most grains show well-developed quartz pressure shadows.

One of the most important observations of the petrographic work is that the textures suggest that magnetite was in equilibrium with accompanying phases, including quartz, calcite and siderite, in all rock types from all localities. Therefore, these coexisting minerals can be used as pairs for oxygen isotope geothermometry.

Electron microprobe

We analysed samples using energy dispersive electron microprobe analyses at the University of Auckland and wavelength dispersive electron microprobe analyses at the University of Michigan. Both sets of analyses demonstrated that magnetite from all localities and geological settings is essentially pure Fe_3O_4 (Nadoll et al., 2007). However, lower detection limits from the University of Michigan microprobe allowed us to demonstrate that magnetite from the Belt Supergroup does contain low concentrations of some trace elements.

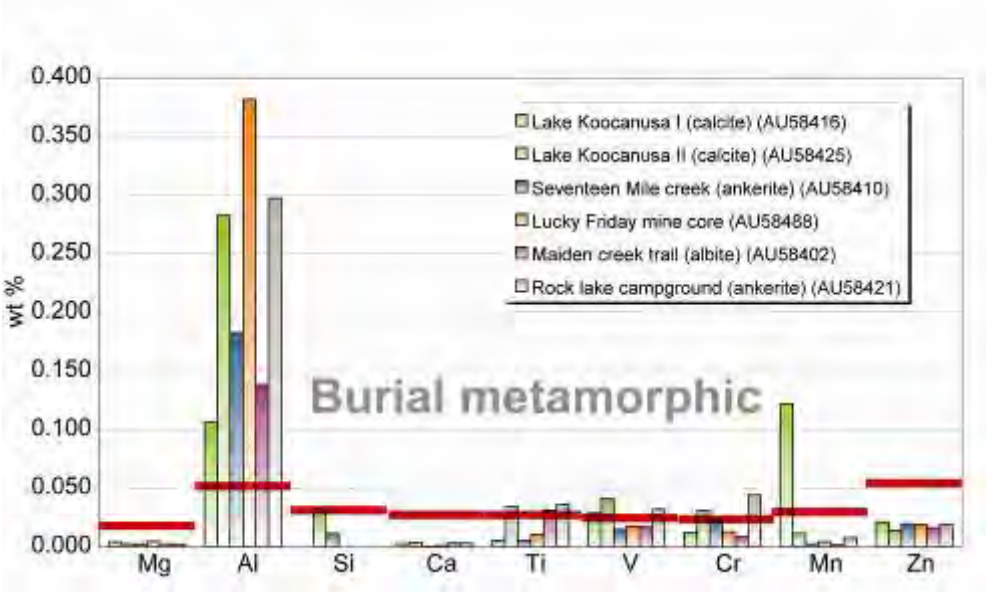

Figure 2. Electron microprobe results (University of Michigan microprobe) for a selection of burial metamorphic magnetite samples. Red lines represent the respective detection limit. The complete electron microprobe dataset can be found in Appendix A.

Most of the values for Zn (0.0563 wt%), Mg (0.0124 wt%), Ca (0.0186 wt%), and Si (0.0297 wt%) lie below their corresponding detection limits. The detection limit for Mg is only exceeded in magnetite from the pyroxenite sample from Vermiculite Mountain. Two hydrothermal vein samples from the Coeur d'Alene district contain the only magnetite with Ca and Si values that exceed the detection limits for those elements.

Only a few samples of magnetite from burial metamorphic and hydrothermal vein samples show values that exceed the detection limits for Ti, V and Cr (Fig. 1; Ti: 0.0186 wt%, V: 0.0162 wt%, Cr: 0.0146 %). Similarly, magnetite from igneous intrusions and several sediment hosted copper deposit samples provided analyses whose Ti and V values significantly exceeded the detection limits of the electron microprobe.

The University of Michigan microprobe analyses show that differences do exist in the trace element composition of magnetite form the different geologic settings, but these differences are very minor, and as a consequence, do not show any clear trends or patterns. Appendix A contains a complete dataset of the electron microprobe analyses.

Wüstite

One vein sample from the Coeur d'Alene district contains wüstite that coexists with magnetite (Nadoll and Mauk, 2008). The wüstite has a composition that is essentially pure FeO, and Appendix B contains related electron microprobe results.

Laser Ablation Inductively Coupled Plasma Mass Spectrometry

Laser ablation inductively coupled plasma mass spectrometry (LA-ICP-MS) analyses provide considerably lower detection limits than electron microprobe analyses, and therefore provide better resolution for trace element concentrations. Our LA-ICP-MS data show minor but distinct differences in the geochemistry of magnetite from different geologic settings. Magnetite from Coeur d'Alene mining district veins is depleted in Cr, Ni, and Co compared to magnetite from other settings. Magnetite from Coeur d'Alene mining host rocks is also depleted in a number of elements (Mn, Co, Zn, V), whereas Cr, Ni, and Ti show values similar to those in magnetite from igneous, burial metamorphic, and sediment-hosted Cu settings.

Many of the elements that we measured using LA-ICP-MS have concentrations that show a widespread range of values among magnetites from all geologic settings. Some elements show a wide range of concentrations even within the same sample.

Magnetite from the Spar Lake sediment hosted stratiform copper deposit has copper values that are clearly related to micro-inclusions of copper sulfides rather than representing copper in the magnetite structure. In fact, LA-ICP-MS analyses revealed many micro-inclusions of silicates, sulfides, and apatite. Figure 3 shows one analysis with an apatite inclusion that can be distinguished by increasing values for several elements, particularly Ca and P. Despite these changes in the overall chemistry, the values for Mn and V, among others important for magnetite, don't seem to be affected and might still contribute useful data. However, other inclusions, such as sulfide minerals, affect the measured metal contents more significantly, and we therefore generally excluded the areas obviously containing inclusions and only processed the rest of the data (green area in Fig. 3). On the one hand, these inclusions present a difficulty for data processing, but on the other hand the occurrence or absence of these inclusions and their specific mineralogy may also provide useful information that can be used to discriminate samples.

Appendix C provides a complete dataset of the LA-ICP-MS analyses.

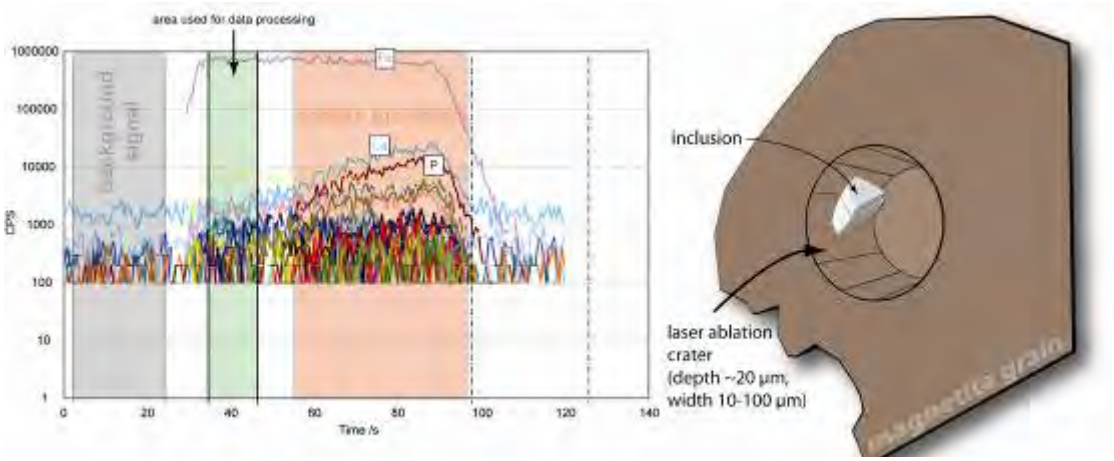

Figure 3. Left: Laser ablation signal showing an apatite inclusion and areas used for data processing. Right: Magnetite grain with laser ablation crater and inclusion affecting the signal.

Factor analysis

The data obtained with LA-ICP-MS were used for factor analysis to examine any underlying relations between elements and to detect spinel element clusters. Factor analysis is a good approach to determine clusters, patterns and elements of interest within large datasets. Magnetite from the four main geologic settings was analyzed for a selection of spinel elements (Mg, Al, Ti, V, Cr, Mn, Co, Ni, Cu, Zn, Ga, and Pb) and for the bulk chemistry. The combination of chemical and geological discrimination created a total of 7 different datasets. This report presents the datasets that are restricted to the spinel elements because they have the highest importance and show the most unambiguous trends. Appendix D contains a complete collection of these datasets.

The range and variance of element concentrations can be used as an indicator for dubious values that may be attributed to inclusions rather than representing trace element concentrations of magnetite. For factor analysis, we excluded elements that showed no variance, or whose concentrations fell below the limits of detection for certain geologic settings (e.g. P, Nb and Sm for the igneous samples). Scree plots illustrate the importance of the different factors, or components (Figure 4). In general, factors with eigenvalues below 1 can be regarded as negligible. Scree plots typically show a distinct break between the steep slope of the large factors and the gradual trailing of the rest (the scree; Fig. 4a). The values in the rotated component matrix determine the degree of correlation between different elements. The rotated component plots give a first impression of which elements are clustered and which of these clusters have the highest significance for the geochemistry of magnetite. The more concentrated, isolated, and further away from the centre they are, the more significance can be ascribed to them.

Figures 4a and 4b show the scree plot and the corresponding rotated component matrix for spinel elements for all geologic settings. Two factors, or clusters, of spinel elements are prominent. Factor 1 is a cluster of Mg and Mn and factor 2 comprises Cr and Zn. Factor 3, 4, and 5 include V, Ti, Co, Ni, and Cu. Their individual and overall clustering is less pronounced, which indicates that these elements have less significance within this dataset than factor 1 and 2. Because this dataset incorporates all geologic settings, some clusters might be subdued or elusive.

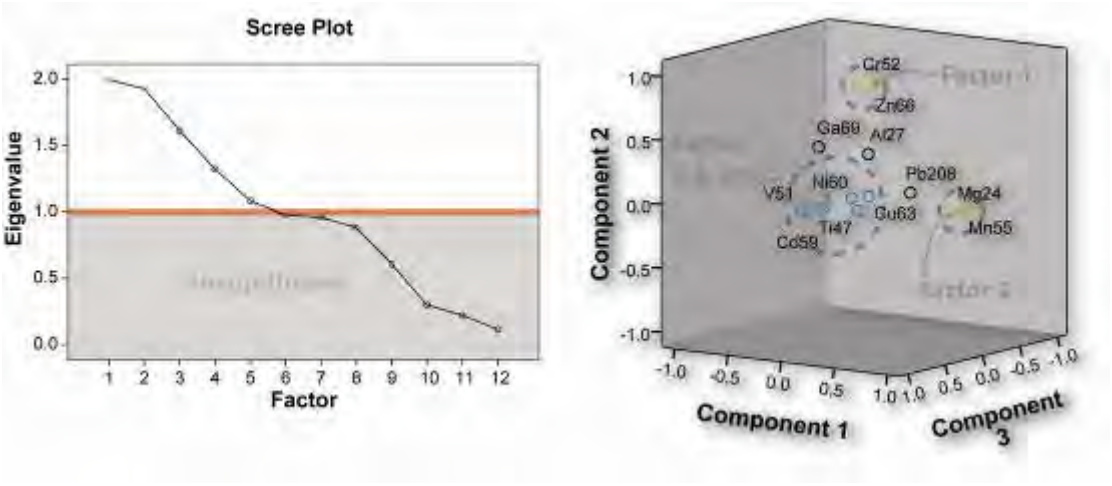

Figure 4a, b. Scree plot (a) and rotated component matrix (b) for all geologic settings but restricted to a selection of spinel elements. Factors with eigenvalues below 1 can usually be neglected. The complete dataset including all geologic settings can be found in Appendix D.

Spinel elements - bulk dataset

The slope in the scree plot is not very pronounced, indicating that there may be too many interfering factors. However, the rotated component matrix indicates two strong relationships between 1) Mg and Mn, and 2) Cr and Zn. Factors three, four, and five show only moderate correlation among V, Ti, Co, Ni, and Cu.

Spinel elements - Burial metamorphic

According to the scree plot, the first three factors appear to be the most important. The first factor is a slightly diffuse correlation between Mg, Al, Mn, Co, and Pb, wherein Mg and Pb show the strongest positive correlation. Vanadium and Ga, with a positive correlation and Ni, with a negative correlation represent the second factor. Interestingly, factor three corresponds with what the factor analysis of the complete dataset already suggested, a strong correlation between Cr and Zn.

Table 1 shows the mean trace element values in ppm for the different geologic settings. The values for the burial metamorphic setting are used as an arbitrary standard against which the mean trace element values of the other geologic settings are compared.

Table 1. Mean trace element values for the different geologic setting.

burial metamorphic

	N	Mean
Al27	61	703
Cr52	61	617
Ti47	61	592
Mn55	61	281
V51	61	281
Zn66	61	193
Ni60	61	103
Co59	61	45
Mg24	61	40
Ga69	61	10
Cu63	61	3
Pb208	61	2

Coeur d'Alene vein

	N	Mean
Mn55	25	1974
Ti47	25	1093
Mg24	25	920
Al27	25	693
Pb208	25	98
V51	25	76
Cr52	25	57
Zn66	25	51
Ni60	25	36
Cu63	25	23
Co59	25	4
Ga69	25	3

Coeur d'Alene host rock

	N	Mean
Al27	52	607
Ti47	52	257
V51	52	145
Ni60	52	102
Zn66	52	44
Mn55	52	44
Cr52	52	43
Co59	52	24
Mg24	52	17
Ga69	52	4
Pb208	52	2
Cu63	52	0

sediment-hosted Cu

	N	Mean
Cu63	67	3492
Ti47	67	541
Al27	67	504
Cr52	67	473
V51	67	454
Mn55	67	184
Zn66	67	112
Mg24	67	46
Co59	67	23
Ni60	67	18
Ga69	67	10
Pb208	67	3

igneous

	N	Mean
Cu63	16	2822
Cr52	16	1820
Ti47	16	1209
V51	16	1206
Al27	16	1078
Mg24	16	894
Mn55	16	854
Zn66	16	278
Co59	16	161
Ni60	16	70
Ga69	16	14
Pb208	16	3

Spinel elements - Sediment-hosted Cu

The component plot for magnetite from sediment hosted stratiform copper deposits shows elements that are rather scattered and no cluster particularly stands out. The scree plot also shows a rather feebly sloping graph. Nevertheless, four factors are reasonably well pronounced. The first factor has a relationship between V and Mn. The second factor, with a negative correlation between Co and Zn is an interesting statistical relationship, but does not resolve any questions regarding different magnetite species. The third factor is similar to the first factor of the burial metamorphic setting and might represent a universal factor, which can be found in all geologic settings with slight differences. Finally, copper can not be found in any of the factors.

There are only subtle overall differences between magnetite from the sediment-hosted Cu and the burial metamorphic settings (Table 1). The sediment-hosted Cu magnetite seems to have slightly less Al, Cr and Mn than the burial metamorphic magnetite, but higher V contents. Copper is excluded here because in

this geologic setting Cu is clearly related to sulfide mineral inclusions and not the magnetite.

Spinel elements - Igneous

The factor analysis results are quite pronounced for magnetite from igneous settings, and the factors comprise multiple elements. The first factor consists of Al, Cu, Ga, and Pb with a negative correlation towards V, Co, and Ni. The second factor indicates moderate to strong positive correlations among Mg, Ti, V, Mn, Co, and Ni. The negative correlation in the first factor towards the elements of the second factor suggests two discrete groups of magnetite with different geochemistry. A third factor contains Cr, Zn, and Ga. Overall, this setting shows the most precipitous slope together with a pronounced clustering and the most unambiguous indication of magnetite with different geochemistry in the same rock.

Magnetite from igneous rocks has the highest overall trace element contents of magnetite from all geologic settings and is markedly enriched in Cu, Cr, Ti, and V, Mn, Mg. Furthermore the extremely low mean value for Pb indicates that this element is not of particular significance for the first factor (Table 1).

Spinel elements - Coeur d'Alene veins

The scree plot indicates that the first three factors have the highest relevance for magnetite from veins from the Coeur d'Alene district. The first factor contains a number of elements that seem to be subdivided into two groups. (I) Vanadium and Co form one subcluster and (II) Cr, Ni, and Ga form the other one. The other two nicely clustered factors are: 2) Ti, Cu, (Co), and 3) Mg, Mn, (Zn). The latter two factors can also be found in the complete dataset analysis, which is evidence for their overall significance.

Magnetite from the Coeur d'Alene veins have the highest overall value for Mn. Titanium, Mg and Pb values are also elevated in comparison to the burial metamorphic standard (Table 1). On the other hand, Cr, V, Zn, and Ni are depleted in comparison to the burial metamorphic setting.

Spinel elements - Coeur d'Alene host rock

Magnetite from Coeur d'Alene host rocks shows signatures similar to magnetite from burial metamorphic sedimentary rocks elsewhere. A strongly pronounced first factor with Mg, Mn, and Co and a second one with Mg, Al, and Ga clearly point out the similarity between the two settings. However, Zn and Ni, which are present in magnetite from Coeur d'Alene district host rocks, cannot be found in the burial metamorphic setting. Another interesting difference is the lack of Pb in magnetite from Coeur d'Alene host rocks despite the fact that galena is a major ore mineral in the district.

The above-mentioned observation that the geochemical signature of magnetite from Coeur d'Alene host rocks is relatively similar to the geochemical signature of magnetite from burial metamorphic rocks seems to be confirmed when looking at the mean trace element values in Table 1. However, the trace element values of magnetite from Coeur d'Alene district host rocks are slightly lower than those for the

burial metamorphic magnetite. In particular Zn, V, Mn, Ti, and Cr are depleted within Coeur d'Alene host rock magnetite.

Oxygen isotope analyses

We analyzed 20 magnetite samples and co-existing phases such as siderite, calcite and quartz from Spar Lake, the Coeur d'Alene mining district, and burial metamorphic host rocks (Fig. 5). Oxygen isotope values for magnetite from the Upper Revett at Spar Lake range from 0.29‰ to 3.29‰ relative to SMOW. Two clusters exist, one with a mean of 0.5‰ and another one with a mean value of 2.9‰. Co-existing intergranular calcite yields oxygen isotope values between 11.7‰ to 12.8‰. Calcite-magnetite oxygen isotope geothermometry yields calculated temperatures for the Spar Lake deposit that range from 359°C to 432°C. These calculated temperatures reflect maximum burial metamorphic temperatures of approximately 425°C for this area, rather than ore forming conditions, which reached temperatures of around 170°C (Hayes, 1990).

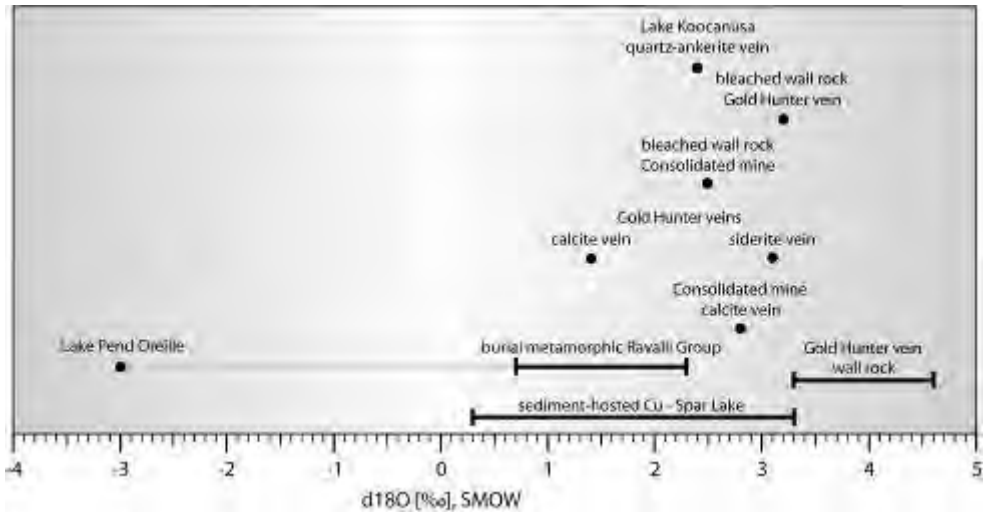

Figure 5. Range of oxygen isotope values for magnetite from different geologic settings.

Two samples of vein magnetite from the Gold Hunter deposit in the Coeur d'Alene district yield $\delta^{18}O$ values of 1.4‰ and 3.9‰. The first sample is associated with calcite that has an oxygen isotope value of 19.7‰, and the second sample is from a siderite vein whose siderite yields a $\delta^{18}O$ value of 16.7‰. Temperature calculations yield 220°C for the calcite/magnetite pair and 342°C for the siderite/magnetite pair. Magnetite from a calcite vein in the Consolidated Silver mine in the Coeur d'Alene district yields $\delta^{18}O$ values of 2.8‰ for the magnetite and 12.8‰ for co-existing calcite. This yields a calculated temperature of 407°C, which is greater than the 250-350°C that most workers accept as the temperature of formation for the widespread siderite veins that host most mineralization in the district (e.g. Leach et al., 1988).

Samples from a hydrothermal quartz-ankerite vein at Lake Koocanusa yield $\delta^{18}O$ values of 2.4‰ for magnetite and range between 13.1‰ and 13.9‰ for quartz. The corresponding calculated temperatures are 381°C and 400°C.

Oxygen isotope values of magnetite from Coeur d'Alene district host rocks range from 3.2‰ to 4.6‰. Associated siderite yields $\delta^{18}O$ values between 17.0‰ and 17.2‰ which leads to calculated host rock temperatures of 296°C to 327°C. In comparison, burial metamorphic magnetite samples from Lake Koocanusa, Rock Lake and Seventeen Mile Creek yield $\delta^{18}O$ values of 2.3‰, 2.0‰, and 0.7‰ respectively. Another sample of magnetite from burial metamorphic rocks at Lake Pend Oreille yields a $\delta^{18}O$ value of -3.3‰, which is clearly an outlier, but we include it here for the sake of completeness.

In summary, oxygen isotope analyses have provided valuable temperature constraints for different vein types inside and outside the Coeur d'Alene mining district, and clearly indicate that magnetite from the Spar Lake sediment-hosted Cu deposit is metamorphic or re-equilibrated during metamorphism. Furthermore, the success of oxygen isotope geothermometry with burial metamorphic rocks raises the intriguing possibility that regional studies of magnetite-quartz pairs from burial metamorphic rocks at the same stratigraphic horizon may be useful to reconstruct metamorphic histories across different thrust sheets in the Belt Terrane.

Discussion & Conclusion

Microprobe analyses indicate that magnetite from all geological settings in the Belt Supergroup is essentially pure Fe_3O_4. In spite of this, the low detection limits afforded by LA-ICP-MS analyses have allowed us to document the trace element geochemistry of magnetite from different geological settings. Factor analysis has revealed small differences among magnetite samples from different geologic settings.

Data derived by factor analysis must be closely examined to avoid misinterpretation. For example, Cr, Co, and Ni are part of possible spinel related clusters in the Coeur d'Alene vein dataset. When this is being put into context with the LA-ICP-MS data (see Appendix C), the initial interpretation has to be revised. The LA-ICP-MS plots clearly show that Cr, Co, and Ni are depleted in the Coeur d'Alene vein samples and are therefore of minor significance for this dataset. Another example is the bulk chemistry of magnetite analyses from the sediment-hosted Cu dataset, which shows that the range and variance for Cu, as well as for Ag, and S are questionably high. Copper, Ag, and S form a distinctive cluster within the data for the sediment hosted Cu deposits. The clustering of these elements clearly indicates that Cu and Ag are related to sulfide inclusions and are not genuine trace elements in magnetite grains. The first factor of this data set may be related to spinel geochemistry because of the occurrence of Ti. However, it also yields elements that are more likely related to inclusions (Nb, Sb, W, Th, and U). In addition to the above mentioned Cu-Ag-sulfide cluster in this data set, there are several clusters that clearly represent spinel elements, but are, on an overall scale, not very pronounced.

The Kaiser-Meyer-Olkin Measure of Sampling Adequacy, which is a statistic that indicates the proportion of variance in variables that might be caused by underlying factors, has an average value of 0.53 for the factor analyses for the different settings (max 0.702 - Coeur d'Alene veins; min 0.424 - igneous). Values

lower than 0.50 indicate that the factor analysis probably will not be very useful for statistical examination, so some datasets need to be treated with extra caution. Bartlett's test of sphericity tests whether or not a dataset is suitable for structure detection. Small values (less than 0.05) of the significance level indicate that a factor analysis may be useful with the data. All datasets herein have a value of 0.00 for the Barlett test, which suggests valid and significant analyses.

The most pronounced overall signature found by factor analysis seems to be a Mg, Mn factor (± other spinel elements) that can be recognized in the Coeur d'Alene district as well as in igneous rocks. Another very pronounced factor comprises Cr and Zn and can be found in the burial metamorphic as well as in the igneous setting. The sediment-hosted Cu setting has the weakest overall signature, but can be recognized by the presence of copper sulfide inclusions.

Oxygen isotope values for magnetite from the Spar Lake sediment hosted stratiform copper deposit and the corresponding calculated temperatures of 359°C to 432°C clearly indicate a burial metamorphic origin or overprint rather than ore forming conditions, which reached temperatures of approximately 170°C (Hayes, 1990). Oxygen isotope geothermometry of magnetite-siderite pairs in veins and host rocks of the Coeur d'Alene district yields temperatures that are broadly consistent with previous determinations of vein formation temperatures of around 250-350°C (e.g. Leach et al., 1988; Landis and Hofstra, 1991) although calcite-magnetite veins yield calculated temperatures that lie outside of this range.

In summary, available data are consistent with formation or re-equilibration of magnetite in different geological settings of the Belt Supergroup during regional metamorphism (Nadoll et al., 2007). This may reflect regional-scale burial metamorphism or regional magmatic-thermal events related to the East Kootenay orogeny at <1370 Ma (Doughty and Chamberlaine, 1996). Minor differences in the geochemistry of magnetite may reflect differences in the geochemistry of the host rock, or in the case of vein magnetite, may reflect the composition of the hydrothermal fluid. The exception to the above is magnetite from plutonic rocks in the region, which is also essentially pure Fe_3O_4 due to subsolidus re-equilibration of magnetite, similar to what has been reported for magnetite from plutonic igneous rocks elsewhere (Lindsley, 1991b).

Finally, we note that the wüstite grain in one sample of magnetite from a siderite vein in the Coeur d'Alene district must be a metastable phase. Our oxygen isotope geothermometry data are consistent with previous work that indicate that the Coeur d'Alene district veins formed under relatively low temperature and low pressure conditions (250-350 °C and 1-3 kbars, (e.g. Leach et al., 1988)) and are thereby far below the 570°C minimum temperature of wüstite formation (Shen et al., 1983; Lattard and Evans, 1992). Furthermore, siderite is stable to temperatures up to 363 °C, and therefore the existence of wüstite in a siderite vein precludes its formation as a primary phase. This may be the first description of metastable wüstite that is not a product of decomposition of primary wüstite and has not formed through biologically mediated alteration of deep sea hydrothermal iron minerals (Baturin and Dubinchuk, 1984).

Acknowledgments

We thank Tim Hayes, Steve Box, Art Bookstrom, and Al Hofstra for valuable assistance and feedback. We thank Alan Koenig for LA-ICP-MS analyses, and for many discussions of our analytical work. Research supported by the U.S. Geological Survey (USGS), Department of the Interior, under USGS award number 06HQGR0173. The views and conclusions contained in this document are those of the authors and should not be interpreted as necessarily representing the official policies, either expressed or implied, of the U.S. Government.

References

Baturin, G.N., and Dubinchuk, V.T., 1984, Manganosite and wustite in iron-manganese nodules of the Pacific ocean: Okeanologiya, v. 24, p. 311-315.

Boetcher, A.L., 1967, The Rainy Creek alkaline-ultramafic igneous complex near Libby, Montana, part I: Ultramafic rocks and fenite: Journal of Geology, v. 75, p. 526-553.

Doughty, P.T., and Chamberlaine, K.R., 1996, Salmon River arch revisited: New evidence for 1370 Ma rifting near the end of deposition in the Middle Proterozoic belt basin: Canadian Journal of Earth Science, v. 33, p. 1037-1052.

Harrison, J.E., and Cressman, E.R., 1993, Geology of the Libby thrust belt of northwestern Montana and its implications to regional tectonics: U.S. Geological Survey Professional Paper 1524, scale 1:125,000.

Harrison, J.E., Kleinkopf, M.D. and Wells, J.D., 1980, Phanerozoic thrusting in Proterozoic belt rocks, northwestern United States: Geology, v. 8, p. 407-411.

Hayes, T.S., 1990, A preliminary study of thermometry and metal sources of the Spar Lake stratabound copper-silver deposit, Belt Supergroup, Montana: U.S. Geological Survey Open-File Report, v. 90-484, p. 30.

Kleinkopf, M.D., 1997, Geophysical Interpretations of the Libby Thrust Belt, Northwestern Montana: U.S. Geological Survey Professional Paper 1546, 2 plates, 22 p.

Landis, G.P., and Hofstra, A.H., 1991, Fluid inclusion gas chemistry as a potential minerals exploration tool: Case studies from Creede, CO, Jerritt Canyon, NV, Coeur d'Alene district, ID and MT, southern Alaska mesothermal veins, and mid-continent MVT's: Journal of Geochemical Exploration, v. 42, p. 25-59.

Lattard, D., and Evans, B.W., 1992, New experiments on the stability of grunerite: Eur J Mineral, v. 4, p. 219-238.

Leach, D.L., Landis, G.P., and Hofstra, A.H., 1988, Metamorphic origin of the Coeur d'Alene base- and precious-metal veins in the Belt Basin, Idaho and Montana: Geology, v. 16, p. 122-125.

Lindsley, D.H., 1991a, Experimental studies of oxide minerals, in Lindsley Donald, H., ed., Oxide Minerals: Petrologic and Magnetic Significance, Volume 25, Reviews in Mineralogy, Mineralogical Society of America, p. 69-100.

—, 1991b, Oxide Minerals: Petrologic and Magnetic Significance, Reviews in Mineralogy, Mineralogical Society of America, 509 p.

Meeker, G.P., Bern, A.M., Brownfield, I.K., Lowers, H.A., Sutley, S.J., Hoefen, T.M., and Vance, J.S., 2003, The composition and morphology of amphiboles from the Rainy Creek complex, near Libby, Montana: American Mineralogist, v. 88, p. 1955-1969.

Nadoll, P., and Mauk, J.L., 2008, The occurrence of wüstite in a hydrothermal silver-lead-zinc vein, Gold Hunter mine, Coeur d'Alene mining district, USA: Australasian Institute of Mining and Metallurgy v. 41th New Zealand Branch Annual Conference Proceedings, p. 401-409.

Nadoll, P., Mauk, J.L., and Box, S.E., 2007, Magnetite in hydrothermal orebodies and host rocks in the Proterozoic Belt Supergroup, USA: A preliminary report: Australasian Institute of Mining and Metallurgy v. 40th New Zealand Branch Annual Conference Proceedings, p. 269-274.

Shen, P., Bassett, W.A., and Lin-Gun, L., 1983, Experimental determination of the effects of pressure and temperature on the stoichiometry and phase relations of wüstite: Geochimica et Cosmochimica Acta, v. 47, p. 773-778.

Appendix A:
Electron microprobe results for Belt Supergroup magnetite samples

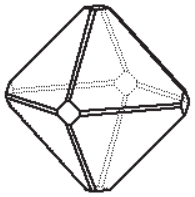

Igneous intrusions

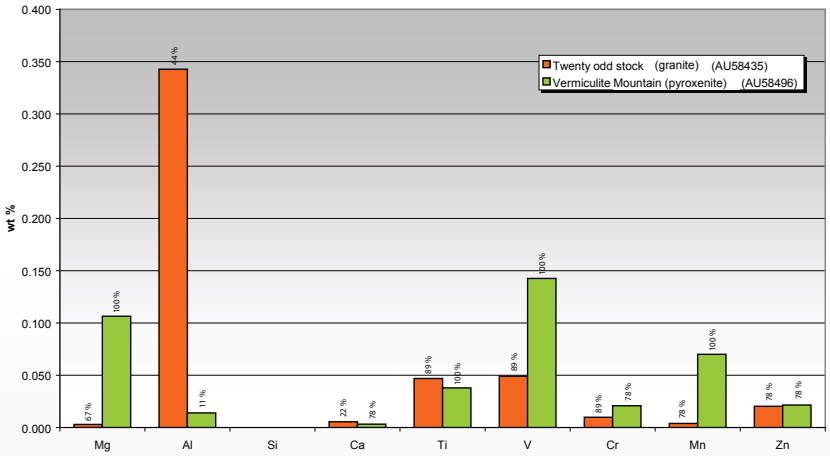

Sediment hosted copper deposit

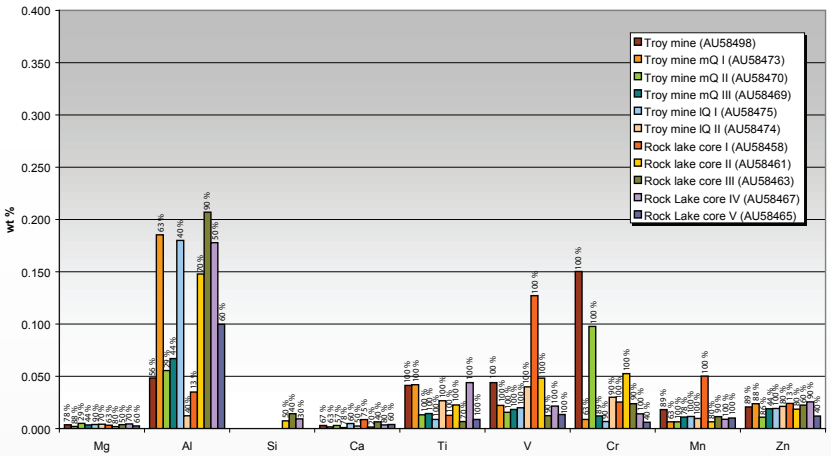

Hydrothermal veins & wall rocks (Coeur d'Alene district)

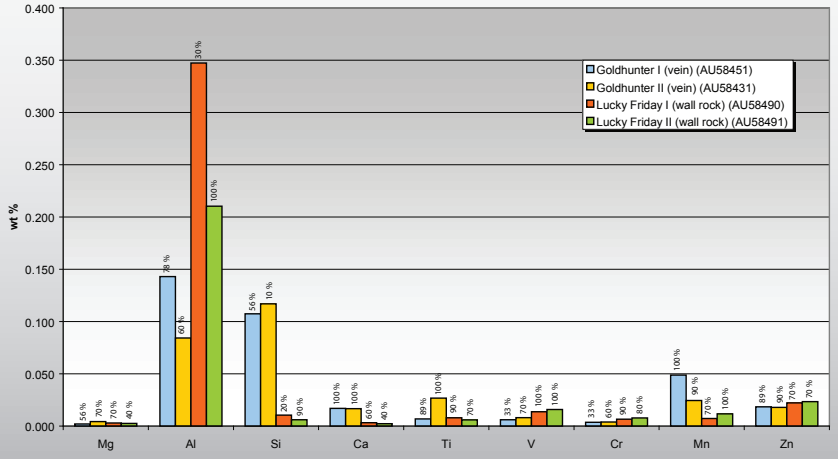

Burial metamorphic sediments

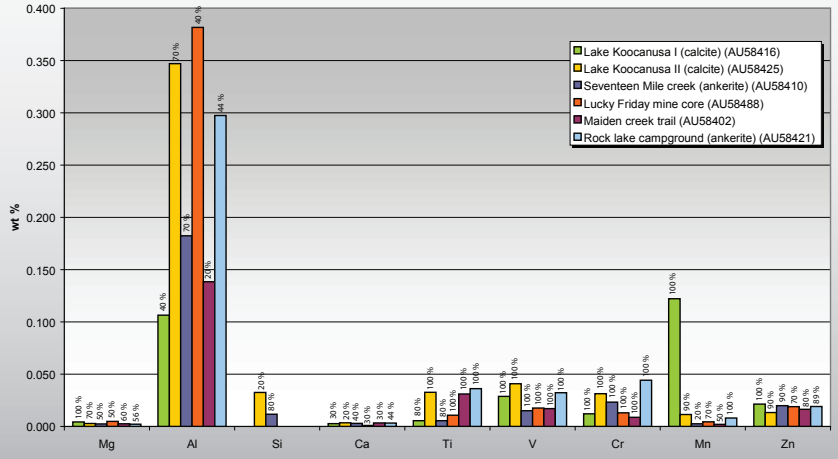

Appendix B: Line scan of AU58492 grain 2 - wüstite/magnetite

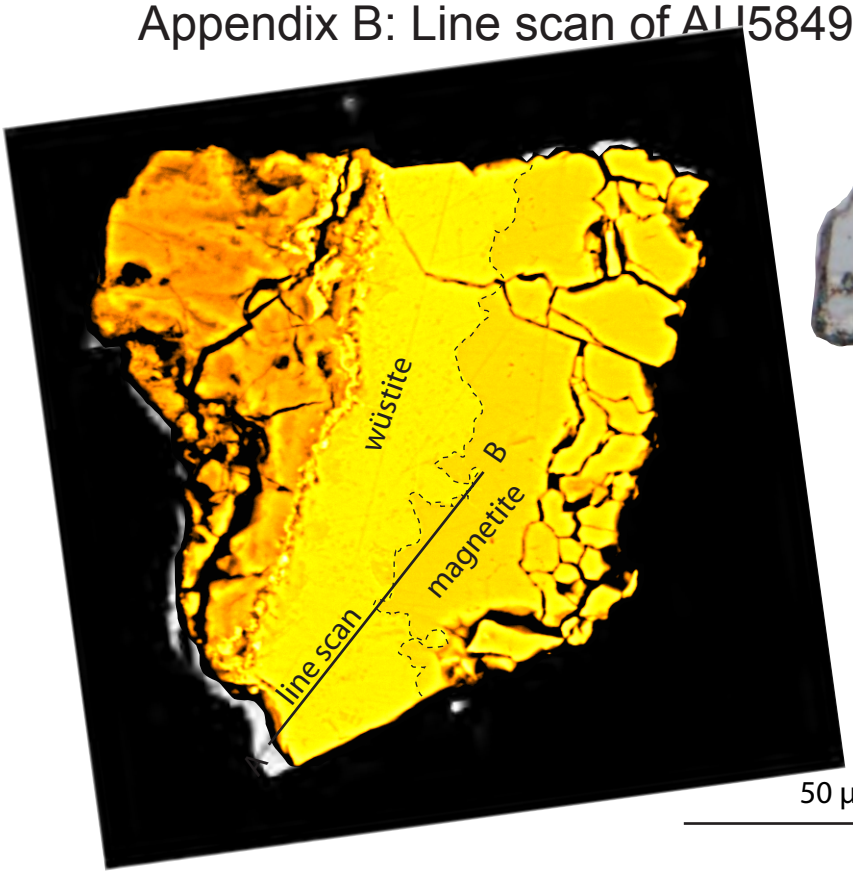

50 µm

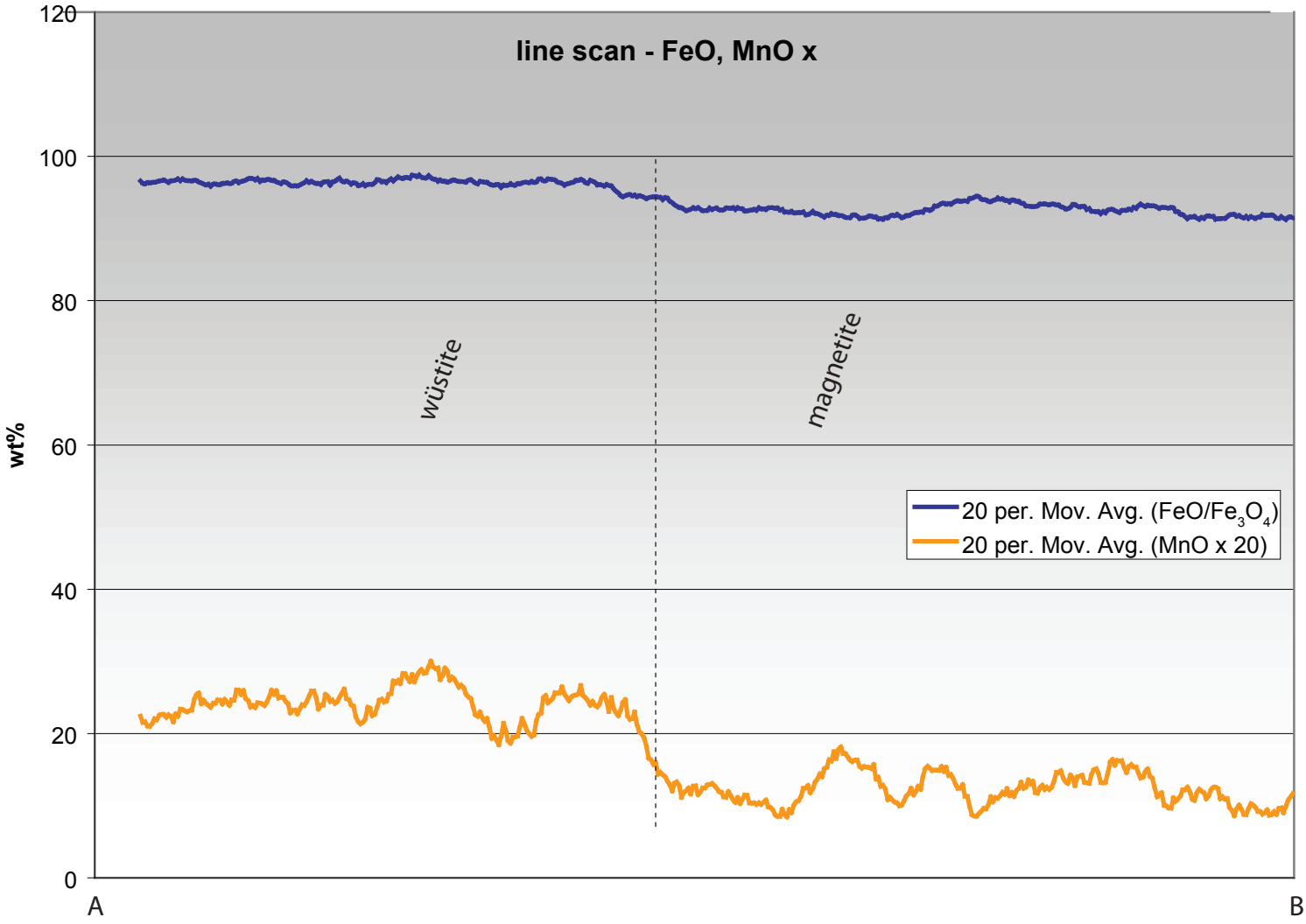

Appendix C: LA-ICP-MS results for Belt Supergroup magnetite samples

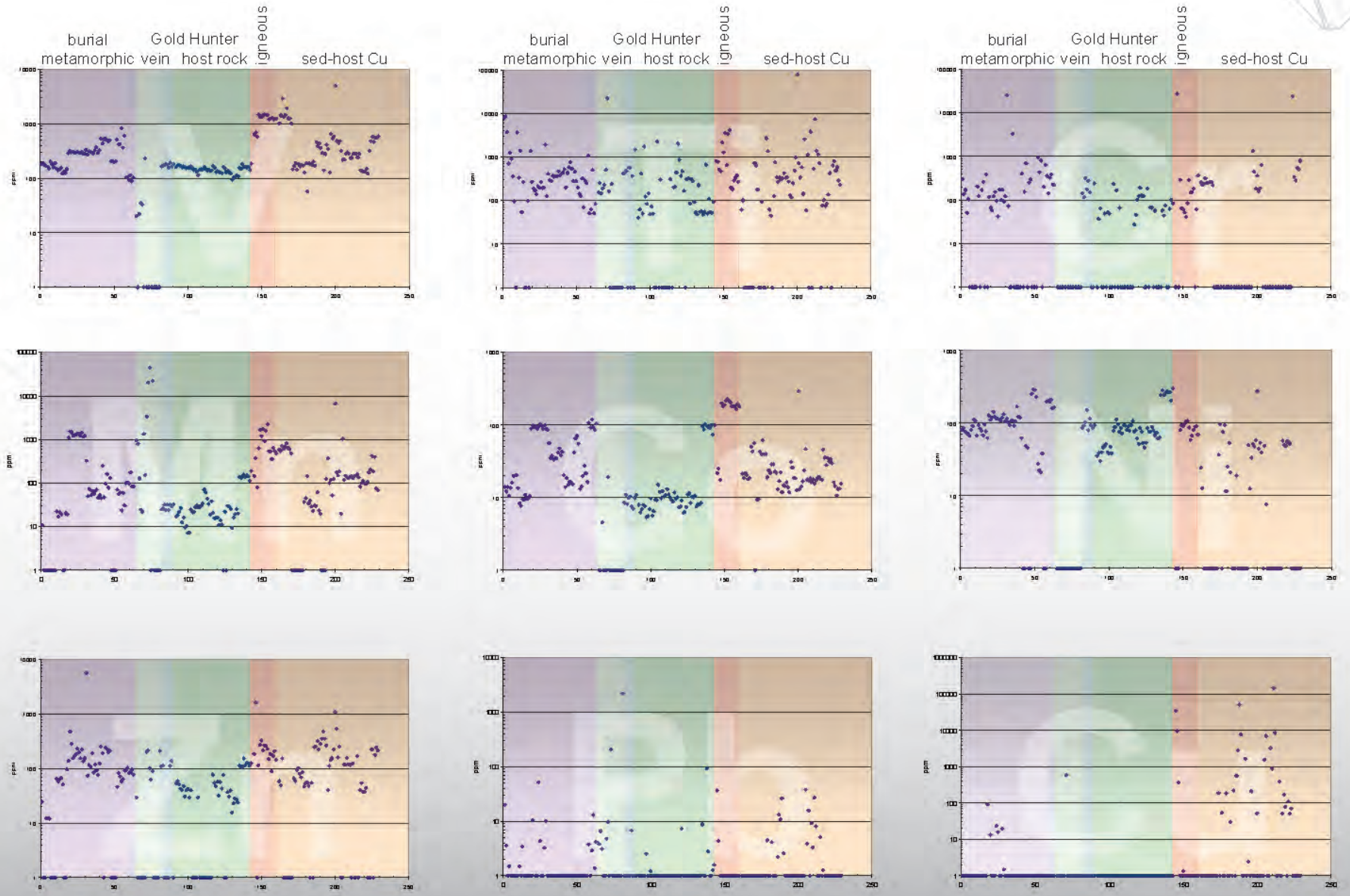

Appendix D: Factor Analysis Results - Spinel Elements (Mg, Al, Ti, V, Cr, Mn, Co, Ni, Cu, Zn, Ga, and Pb)

Complete Data Set

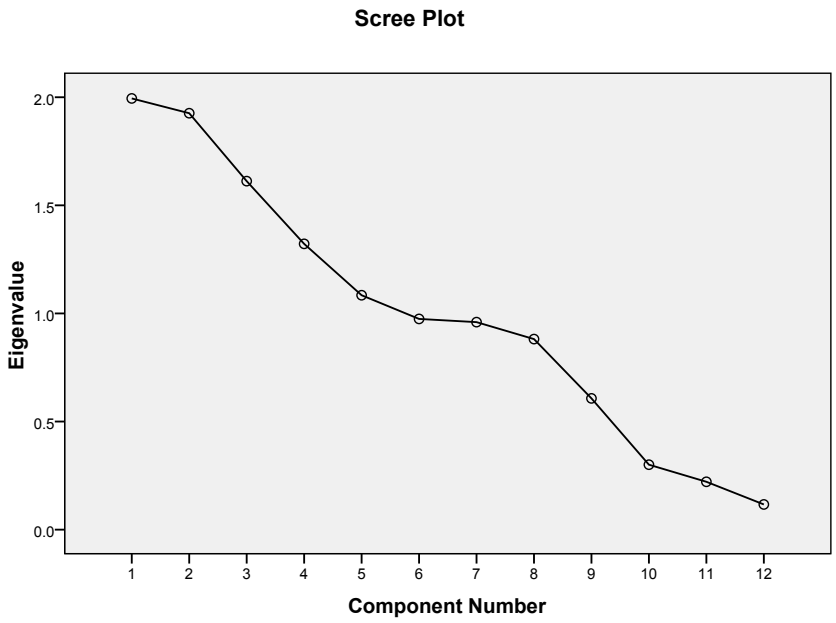

Rotated Component Matrix[a]

	Component				
	1	2	3	4	5
Mg24	.960	-.006	.096	.012	.011
Al27	-.028	.325	-.100	.366	.470
Ti47	.016	-.083	.123	-.002	.679
V51	.042	.042	.894	-.123	.050
Cr52	-.014	.894	.010	-.077	-.009
Mn55	.935	-.004	.009	-.040	-.063
Co59	.117	.027	.716	.590	.038
Ni60	-.110	-.012	.008	.885	-.170
Cu63	-.006	.000	-.073	-.153	.602
Zn66	.068	.865	.021	.094	.002
Ga69	-.143	.441	.404	-.417	-.076
Pb208	.266	.030	-.243	-.029	.059

Extraction Method: Principal Component Analysis.
Rotation Method: Varimax with Kaiser Normalization.
a. Rotation converged in 6 iterations.

Factor	positive correlation	negative correlation
1	Mg, Mn	
2	Cr, Zn	
3	V, Co	
4	Co, Ni	
5	Ti, Cu	

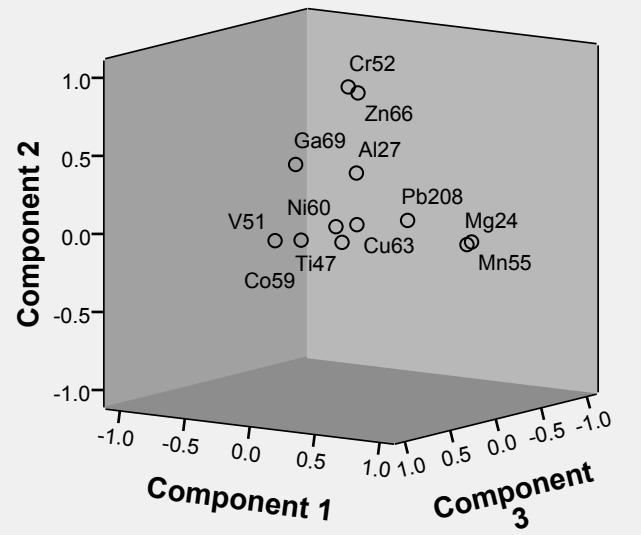

Burial Metamorphic

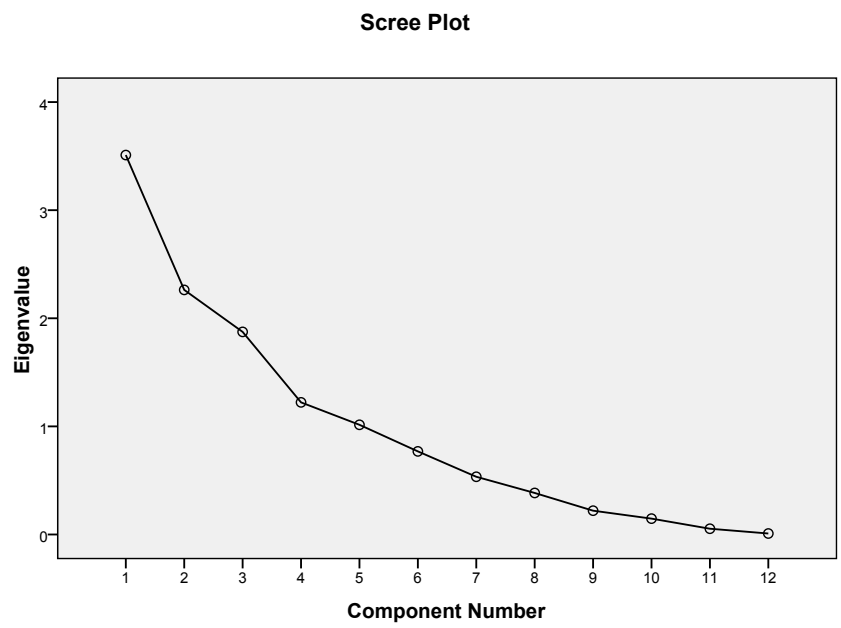

Rotated Component Matrix[a]

	Component				
	1	2	3	4	5
Mg24	.937	-.114	.046	.006	.068
Al27	.661	-.340	.226	-.023	.007
Ti47	.118	-.067	-.038	-.814	-.198
V51	-.040	.887	.049	.088	-.135
Cr52	.016	.023	.993	-.008	-.016
Mn55	.634	.189	-.031	.497	-.090
Co59	.631	-.296	.029	.580	-.245
Ni60	.294	-.770	.024	.270	-.226
Cu63	.152	-.014	-.020	.125	.913
Zn66	.079	.070	.985	.051	-.012
Ga69	.002	.894	.074	.123	-.001
Pb208	.837	.032	-.067	-.145	.269

Extraction Method: Principal Component Analysis.
Rotation Method: Varimax with Kaiser Normalization.
a. Rotation converged in 9 iterations.

Factor	positive correlation	negative correlation
1	Mg, Al, Mn, Co, Pb	
2	V, Ga	Ni
3	Cr, Zn	
4	Co	Ti
5	Cu	

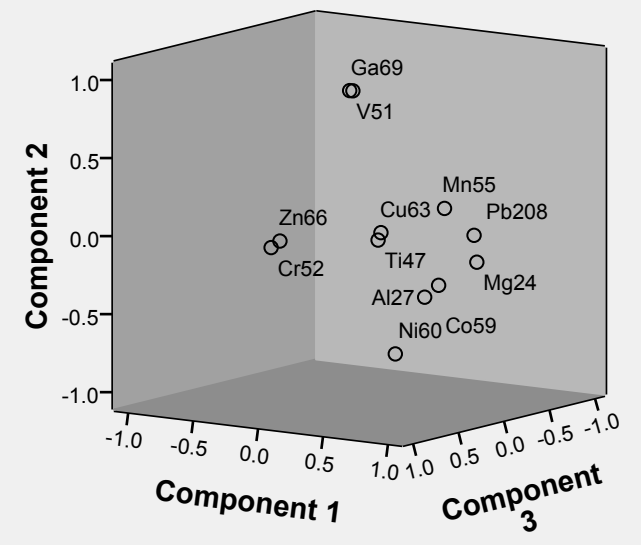

Sediment Hosted Cu

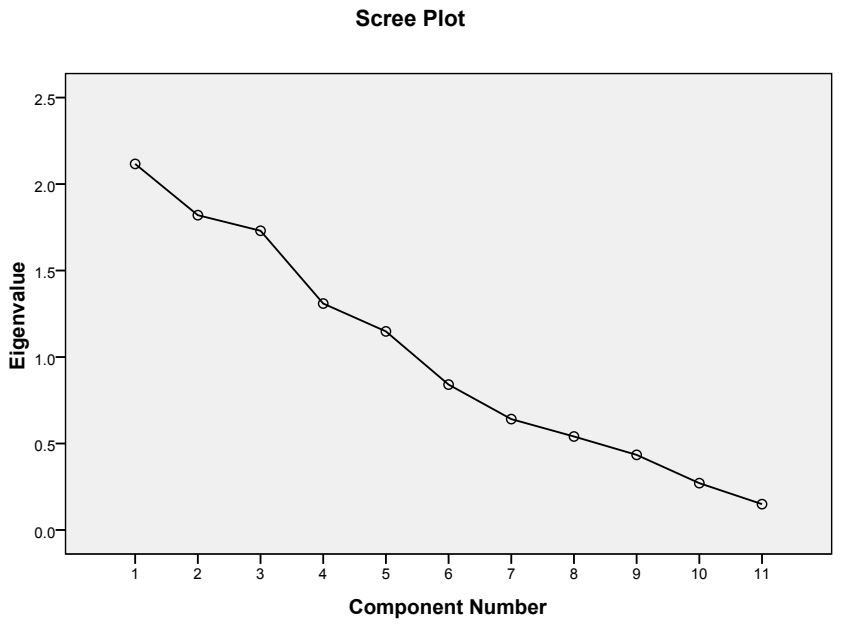

Rotated Component Matrix[a]

	Component				
	1	2	3	4	5
Mg24	.048	.095	.778	-.066	-.146
Al27	-.054	-.215	.763	.060	.115
Ti47	-.128	-.014	-.041	.006	.809
V51	.920	-.039	-.082	.012	-.179
Cr52	.048	.123	-.053	.912	.072
Mn55	.867	.292	.152	.006	.047
Co59	-.026	.815	.038	-.217	-.217
Ni60	-.463	.371	.173	.017	-.469
Zn66	-.179	-.762	.129	-.088	-.152
Ga69	-.056	-.443	.025	.765	-.181
Pb208	.024	.091	.561	-.102	.616

Extraction Method: Principal Component Analysis.
Rotation Method: Varimax with Kaiser Normalization.
a. Rotation converged in 7 iterations.

Factor	positive correlation	negative correlation
1	V, Mn	
2	Co	Zn
3	Mg, Al, Pb	
4	Cr, Ga	
5	Ti, Pb	

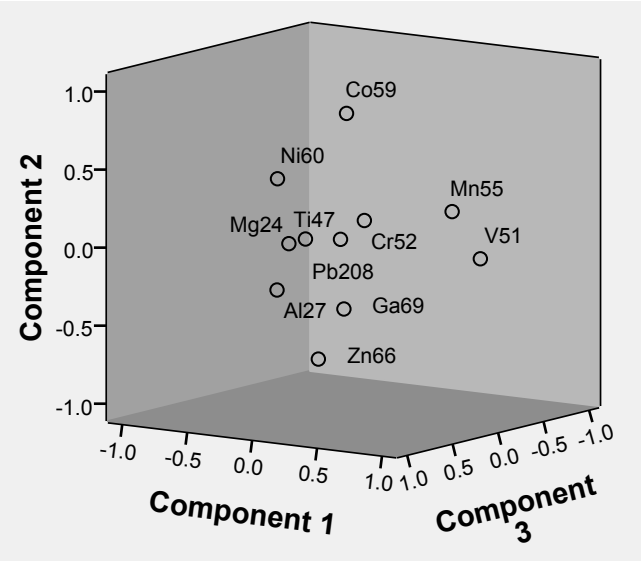

Igneous

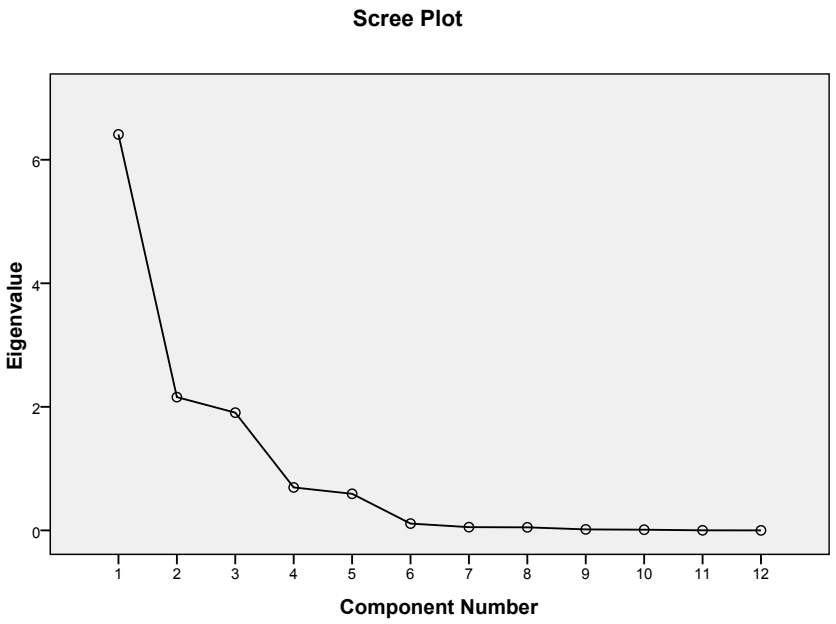

Rotated Component Matrix[a]

	Component		
	1	2	3
Mg24	-.099	.750	-.087
Al27	.941	-.023	.269
Ti47	.054	.887	.060
V51	-.609	.592	-.426
Cr52	.047	-.126	.957
Mn55	-.213	.919	-.053
Co59	-.640	.519	-.482
Ni60	-.606	.583	-.456
Cu63	.957	-.120	.077
Zn66	.054	.046	.951
Ga69	.529	-.112	.706
Pb208	.966	-.099	-.068

Extraction Method: Principal Component Analysis.
Rotation Method: Varimax with Kaiser Normalization.
a. Rotation converged in 4 iterations.

Factor	positive correlation	negative correlation
1	Al, Cu, Ga, Pb	V, Co, Ni
2	Mg, Ti, V, Mn, Co, Ni	
3	Cr, Zn, Ga	

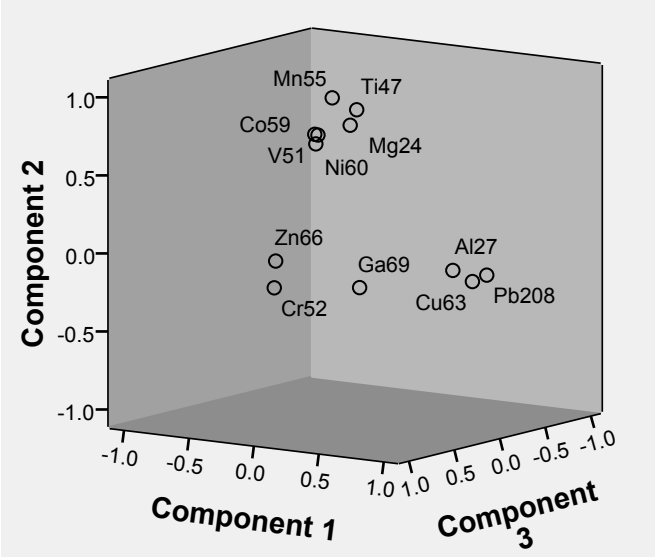

Coeur d'Alene Veins

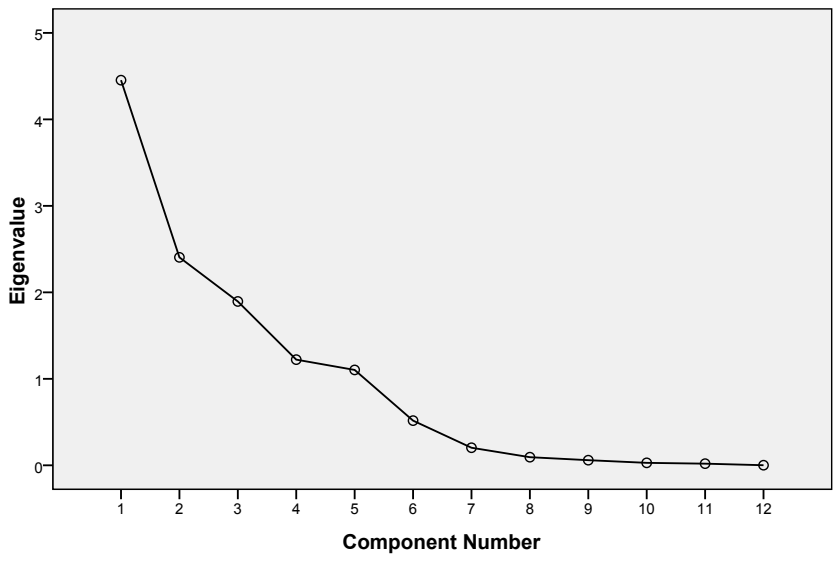

Rotated Component Matrix[a]

	Component				
	1	2	3	4	5
Mg24	-.227	-.049	.934	.129	-.107
Al27	.015	.109	-.137	-.045	.958
Ti47	.005	.993	-.042	-.043	.036
V51	.885	.399	-.146	-.036	.103
Cr52	.824	-.111	-.127	-.139	-.019
Mn55	-.148	-.040	.946	-.045	-.103
Co59	.759	.608	-.131	-.038	.042
Ni60	.964	-.131	-.114	-.020	.020
Cu63	-.028	.993	-.032	-.033	.021
Zn66	.023	-.090	.571	.716	-.002
Ga69	.699	-.174	-.108	-.031	.612
Pb208	-.153	-.025	-.070	.922	-.053

Extraction Method: Principal Component Analysis.
Rotation Method: Varimax with Kaiser Normalization.
a. Rotation converged in 5 iterations.

Factor	positive correlation	negative correlation
1	V, Cr, Co, Ni, Ga	
2	Ti, Co, Cu	
3	Mg, Mn, Zn	
4	Zn, Pb	
5	Al, Ga	

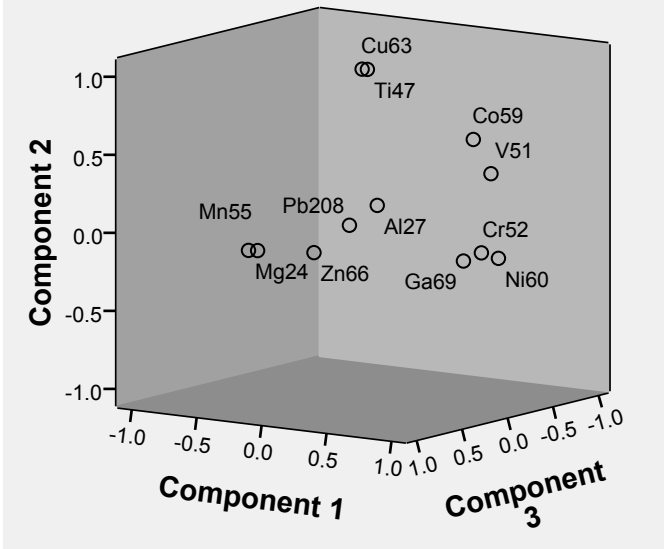

Coeur d'Alene Host Rock

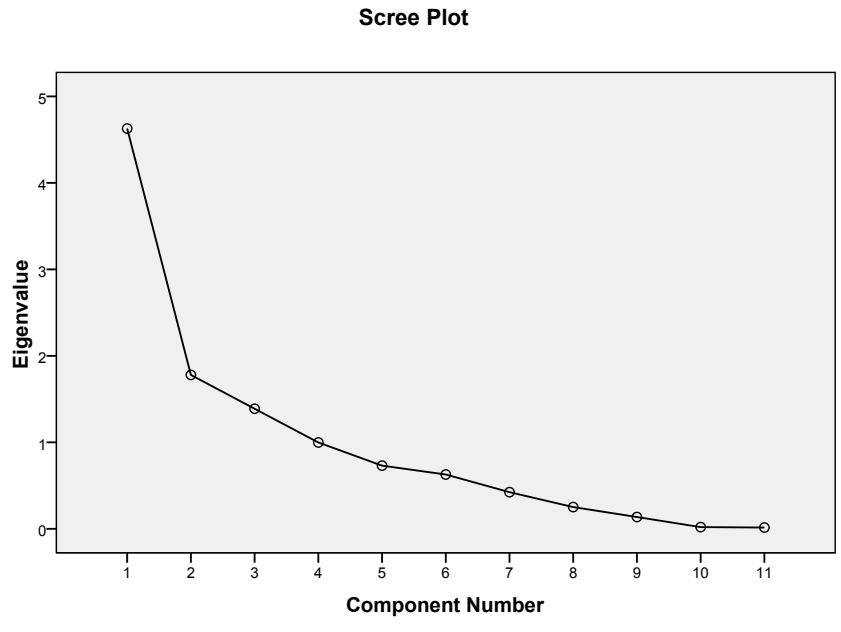

Rotated Component Matrix[a]

	Component		
	1	2	3
Mg24	.621	.635	.185
Al27	.045	.872	.234
Ti47	-.099	.081	.728
V51	.373	.494	-.287
Cr52	.108	.017	.848
Mn55	.934	.093	-.169
Co59	.972	.080	-.086
Ni60	.946	-.014	-.054
Zn66	.862	.219	.016
Ga69	-.519	.566	-.109
Pb208	.451	-.011	.221

Extraction Method: Principal Component Analysis.
Rotation Method: Varimax with Kaiser Normalization.

a. Rotation converged in 4 iterations.

Factor	positive correlation	negative correlation
1	Mg, Mn, Co, Ni, Zn	Ga
2	Mg, Al, Ga	
3	Ti, Cr